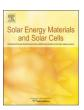
FISEVIER

Contents lists available at ScienceDirect

Solar Energy Materials and Solar Cells

journal homepage: www.elsevier.com/locate/solmat



Liquid phase crystallized silicon - A holistic absorber quality assessment



Paul Sonntag^{a,*}, Matevž Bokalič^b, Natalie Preissler^{a,c}, Daniel Amkreutz^a, Bernd Rech^a, Marko Topič^b

- ^a Institut für Silizium Photovoltaik, Helmholtz Zentrum Berlin für Materialen und Energie GmbH, 12489 Berlin, Germany
- ^b Faculty of Electrical Engineering, University of Ljubljana, 1000 Ljubljana, Slovenia
- ^c PVcomB, Helmholtz Zentrum Berlin für Materialen und Energie GmbH, 12489 Berlin, Germany

ARTICLE INFO

Keywords: Liquid Phase Crystallization Silicon solar cells Thin-film Diffusion length Surface recombination LBIC

ABSTRACT

In this paper, we report on the current status of absorber attributes in Liquid Phase Crystallized Silicon (LPC-Si) cells. To this end, an absorber doping series ($N_D=2\cdot10^{16}$ /cm³ to $7\cdot10^{17}$ /cm³) and an absorber thickness variation (14 and 33 µm) are evaluated. Best cells from the batches for these series showed open circuit voltages up to 640 mV and fill factors above 70%. It is observed that for state-of-the-art cells, thicknesses over 15 µm are not beneficial due to limited diffusion lengths. Lower absorber doping concentrations tend to yield longer intra-grain diffusion lengths (L_{diff}) and better passivated grain boundaries, which may be due to lower impurity precipitation. The longer L_{diff} leads to higher short circuit current densities which over-compensate a decrease in open circuit voltage and fill factor with regards to efficiency. Both front and rear surfaces are sufficiently passivated and at the current status the bulk lifetime has most potential for improvement.

1. Introduction

Many approaches are being pursued to bring down material consumption of Si solar cells using the wafering process by alternative fabrication techniques. These alternatives include classical thin-film technologies like amorphous (a-Si) or microcrystalline (μ -c-Si) Si [1–3], top-down approaches like epitaxial lift-off techniques [4,5] or the liquid phase crystallization (LPC) technology [6]. All of them offer the potential to save material cost while having the advantage to rely on a vast existing knowledge on (crystalline) Si photovoltaics.

LPC of Si absorbers is a zone-melting procedure using a line-shaped energy source to convert an initially amorphous/nano-crystalline precursor to multi-crystalline material directly on a supporting glass with multi-functional thin (200 nm) intermediate layers [6]. In contrast to a-Si/ μ c-Si absorbers [7] LPC-Si absorbers can be up to 40 μ m thick and show grain sizes comparable to multi-crystalline(mc)-Si wafers [8,9]. The technology represents thus a hybrid between wafers and classical bottom-up thin-film technologies. Contrary to that, the elaborate top-down epitaxial lift-off technique uses a high quality mono-crystalline and reusable parent wafer from which absorbers are lifted off and bonded to a substrate [4,5]. Efficiencies of up to 20.6% were presented on 35 μ m Si [10]. With the a-Si/ μ c-Si tandem technology, recently, a 14% cell was achieved [3]. Present efficiencies on LPC-Si are 13.2% on below 15 μ m thick absorbers using an interdigitated back contact (IBC) system and up to 15.9% on full-emitter test structures [11]. LPC-Si has

shown a steep learning curve and progress in recent years, amongst other, thanks to a continuous improvement of the quality of the interface between Si and the supporting glass by an intermediate layer (IL) stack [12,13] and hydrogen plasma passivation techniques [14]. To push performance even further, a thorough material assessment is necessary to find possible levers for improvement. However, many standard wafer characterization methods do not work due to poor signal/ noise ratio (quasi steady state photo conduction, QSSPC) or challenging to evaluate because of substrate effects (photoluminescence, PL). Although it was shown that QSSPC can be measured with under certain circumstances with an altered setup [15], symmetrical lifetime samples can inherently not be processed, because an identical surface treatment as for the buried and inaccessible LPC-Si/supporting glass side cannot be repeated on the other side. Hence, in this publication, we obtain material parameters from illuminated J-V-curves of finished devices and compare them to simulations. The studied devices are bifacial so comparing the two illumination configurations (i) through the glass (superstrate) and (ii) from Si side (substrate) conclusions about the glass/LPC-Si interface quality can be drawn. Furthermore, the change in absorber quality of LPC-Si absorbers with varying phosphorous doping concentration is partly quantified using light beam induced current measurements and J-V measurements.

E-mail address: paul.sonntag@helmholtz-berlin.de (P. Sonntag).

^{*} Corresponding author.

2. Experimental

LPC-Si absorbers were fabricated according to the steps in [11]. For the doping series, 15 μm and for the thickness variation 14 and 33 μm of nominally intrinsic Si were deposited on 1.1 mm Corning Eagle XG glass using high rate electron beam evaporation. Prior to Si deposition a multi-functional intermediate layer (IL) comprised of SiO_x/SiN_x/SiO_x was deposited as described elsewhere [12,13,16]. Amongst others, this IL is crucial for final device performance, since it is the only option to control the passivation and stop impurity diffusion at the glass/LPC-Si interface because later this interface is buried and inaccessible. Subsequent to absorber precursor deposition, a so-called doping layer comprised of a-Si:H(n) was deposited by PECVD to introduce phosphorous (P) dopants. Different final doping concentrations were achieved by varying the phosphine gas flow during deposition. The actual liquid phase crystallization procedure was performed using a line-shaped laser at a wavelength of 808 nm in vacuum [12]. The absorber is molten entirely, allowing the dopants in the doping layer to disperse homogeneously throughout the absorber. Final doping densities between 2.0·10¹⁶ and 7.0·10¹⁷ /cm³ were reached this way. The doping densities were determined by sheet resistance measurements according to

$$N_D = (e\overline{R}_{sheet}\mu_n d_0)^{-1}, \tag{1}$$

 \overline{R}_{sheet} being the averaged sheet resistance of measurements on the entire substrate and the elementary charge e, initial absorber thickness d_0 and majority carrier (electron) mobility μ_n .

The latter was assumed to be 80% of the mobilities of the Masetti model [17] for mono-crystalline Si to account for the poly-crystalline structure. This is in accordance with earlier findings [8,9,14]. An error for the resulting N_D was calculated from the standard deviation of all R_{sheet} measurements. To augment absorber quality a hydrogen plasma treatment [12,14] was performed prior to contact system processing. Finally, interdigitated back contact (IBC) cells using silicon heterojunctions (SHJ) were fabricated on the absorbers for the doping series (Fig. 1(a,c)). Bifacial circular cell test structures (quasi cells, Fig. 1(b,d)) having the lowest doping concentration of the doping series were processed on the absorbers for the thickness variation. Both will be introduced in detail in the following.

2.1. Interdigitated back contact cells

A cross section of an IBC-SHJ unit cell (pitch) is shown schematically in Fig. 1(a) and a photograph of the back (metal) side of a whole cell is depicted in Fig. 1(c). The red dotted line indicates the length of the cross section in (a). The red full rectangle represents the area of the cell (emitter busbar is also counted as cell area). The whole fabrication process in elaborate detail can be found in [11]. In total 44 cells were processed on 4 substrates of doping densities of $2.0 \cdot 10^{16}$, $1.4 \cdot 10^{17}$, $1.7 \cdot 10^{17}$ and $7.0 \cdot 10^{17}$ /cm³. The contact system was co-processed for all cells in the same run and all cells received identical wet chemistry treatment.

2.2. Quasi cell test structures

A schematic cross section of a quasi cell test structure and a topview photograph can be seen in Fig. 1(b) and (d), respectively. The sunpictographs indicate that operation in substrate (front-emitter) and superstrate (rear-emitter) configuration is possible. The cell diameter is 8 mm corresponding to an emitter area of $\sim 0.5 \, \mathrm{cm}^2$. The absorber contact is not passivated and lies outside the defined cell area (cp. red circle in (d)). On one hand the cell has an inherently low fill factor (*FF*) due to a high base series resistance. On the other hand, it is comparably simple to fabricate, fully bifacial and useful for screening short circuit current density (J_{SC}) and open circuit voltage (V_{OC}). The surfaces of the

 $N_D = 2.10^{16} / \text{cm}^3$ absorbers are first cleaned and an a-Si:H(i/p) emitter is formed using low-temperature PECVD. Subsequently, 80 nm ITO is RFsputtered from a ceramic target. The cell area is defined by an adhesive masking tape with circular shape of 4 mm radius made of Kapton®polyimide film with silicone adhesive by Max Steier GmbH & Co. KG. Subsequent to mask-taping the ITO surface, the samples were etched for 10 s in 20% HCl to remove the ITO surrounding the Kapton®dots. In the second etch step of 15-20 s, in a mixture of nitric, phosphorous, and hydrofluoric acid, possible remains of the ITO are removed and the a-Si:H(i/p) emitter is dissolved. After the HF-dip, the samples were thermally coated with 30 nm Ti and 1000 nm Al. The Kapton®dots are temperature resistant up to 270 °C and not affected during all the acidic treatments. Finally, the dots were removed exposing the finished quasi cell test structures depicted in Fig. 1(d). Since all the etching solutions used creep also (on a µm scale) underneath the Kapton®dots an isolation gap is inherently formed during the process between the ITO contact which serves as p-type contact, and the Ti/Al absorber (n-type) contact.

2.3. Methods

Illuminated *J-V* curves were recorded with a dual source solar simulator by Wacom having AAA characteristics [18].

LBIC measurements were conducted using a self-built setup at the University of Ljubljana with a laser of 638 nm wavelength, a spot size below 10 μ m and an x,y,z stage with minimum step width of 1 μ m [19].

Simulations were performed using ASPIN3, a numerical 2D solar cell simulation software, developed at the University of Ljubljana [20].

3. Results

3.1. Doping Series

The main parameters obtained from the recorded illuminated J-V-curves of all the 44 fabricated cells are shown in Fig. 2 except for 3 outliers. The fluctuation in performance leading to the standard deviation of measurements shown as error bars can be attributed to the inhomogeneous mc-Si-like morphology of LPC-Si. We observe a strong decrease of J_{SC} with higher doping (red) and a slight increase of V_{OC} (blue) that seems to decrease again for $N_D = 7.0 \cdot 10^{17} / \text{cm}^3$. The FF tends to increase with doping (orange), while overall conversion efficiency drops steadily (green), following the trend of J_{SC} . Please note that to reach current densities above 30 mA/cm² as in [21,22] a light trapping foil is usually additionally placed on the front glass which has been omitted here. Black circles and triangles are calculated V_{OC} values that will be explained in the discussion section.

Light beam induced current (LBIC) measurements of the best cells with $N_D = 2.0 \cdot 10^{16}$, $1.7 \cdot 10^{17}$ and $7.0 \cdot 10^{17}$ /cm³ were recorded to investigate grain boundary (GB) behavior and evaluate diffusion lengths using a method presented in [23]. The method uses LBIC line-scans to measure the collection signal drop at the absorber contact, where no minority carriers are collected. A measure for this signal drop is the effective diffusion length L_{diff} (taking bulk and interface effects into account) which is obtained by a double exponential fit of the line-scans [23]. The cells on the substrate containing $N_D = 1.4 \cdot 10^{17} / \text{cm}^3$ were omitted, since it is very close to the one of 1.7·10¹⁷/cm³. The complete LBIC 2D collection maps are shown in Fig. 3(a-c). The images were all scaled from 0 to the median of all pixel values. All areas with values above the median appear white. The absorber contacts appear black, since the minority charge carriers generated in this region have to travel laterally to the minority contacts ("electrical shading"). Other areas of reduced collection are due to multi-crystalline nature of LPC-Si (GBs and dislocations). It can be seen that the GBs of the cell with N_D = 7.0·10¹⁷/cm³ are substantially better visible due to a higher signal drop caused by higher recombination than the other two. Diffusion lengths were determined at various places on the cells inside grains at

Download English Version:

https://daneshyari.com/en/article/6534163

Download Persian Version:

https://daneshyari.com/article/6534163

<u>Daneshyari.com</u>